IJESRT

INTERNATIONAL JOURNAL OF ENGINEERING SCIENCES & RESEARCH TECHNOLOGY

Road Sign Detection Using Image Processing & Recognition

L.S. Admuthe[*1], P.G.Bendre[2]

Telecommunication Department Ichalkaranji, Maharashtra, India

pritika2687@gmail.com

Abstract

This paper proposes an automatic road-sign Recognition method based on image segmentation and joint transform correlation (JTC) with the integration of shape analysis. The presented system is universal, which is able to detect traffic signs of any countries with any color and any of the existing shapes(e.g. circular, rectangular, triangular) and is invariant to transformation(e.g. scale translation, rotation, and occlusion). There are three main stages in the proposed algorithm: 1) segmentation by clustering the pixels based on the color features to find the regions of interest (ROIs),2) traffic-sign detection by using two novel shape classification criteria, i.e. the relationship between area and perimeter and the number of sides of a given shape; and 3) recognition of the road sign using FJTC to match the unknown signs with the known reference road signs stored in the database.

Introduction

Automatic detection and recognition of road traffic signs is an essential task for regulating the traffic and guiding and warning drivers and pedestrians. Road signs carry much useful information that is required for piloting, such as to drive the vehicle in the correct lane and at the right speed; to avoid obstacles and potential risks, to notice roadway access, position, and trajectory of other vehicles, pedestrians' movement, road lanes, and status; and to provide information on the current traffic situation, the state of the road, the right of-way, forbidden maneuvers, etc. Similar to advanced driver assistance systems, an assistance system can be developed to help blind pedestrians. Sign detection and recognition can also be useful for highway maintenance so that a human operator does not have to check the presence and condition of the signs; rather, gathering of the traffic-sign position will be done automatically. The goal of this work is to find and classify road signs. In developing a new algorithm for road-sign detection and recognition, we think that any road-sign recognition algorithm should be as general as possible to work with large groups of road signs.

This paper propose a novel framework that can detect road signs with a high success rate. Although there are well-known challenges for sign detection, road signs have well-defined color, shape, size, and position, which aid the detection and recognition tasks. Typically, signs are upright alongside the road, although signs can occasionally appear tilted, and the proposed detector is invariant to rotation, scaling, and translation. Moreover, the system is robust with partial occlusion and variable lighting conditions.

The flow diagram of the proposed system is presented in Section I. The segmentation procedure is described in Section II for the detection of the regions of interest (ROIs). In Section III, the shape classification algorithm for rejecting the detected non road-sign objects, which do not fall under any of the allowed shape categories. The correlation-based matching and recognition process, which classifies the detected ROIs, is described in Section IV.

Proposed Work

The outline of the road-sign recognition algorithm that is presented in this paper is illustrated in Fig. 1. The road signs are detected by using color clues and carrying out geometric property analysis. The system is initiated by clustering the color features for segmentation of the image to search objects with similar colors. The segmented regions are analogized with some possible attributes of a road sign, such as size or aspect ratio, to discard unreasonable objects and retain the candidate ROIs. Next, novel shape classification is performed to categorize the ROIs into different shape groups and also to eliminate the false candidates that do not fall into any of the permitted shape groups. Finally, for recognition, here use the distortion-invariant FJTC technique. In this system, the query image is compared with the composite filters corresponding to reference images in the database, and the reference sign that is most similar to the query sign is returned to the user. The FJTC-based similarity measure used to compare two images is efficient enough to match similar signs and to discriminate dissimilar sign

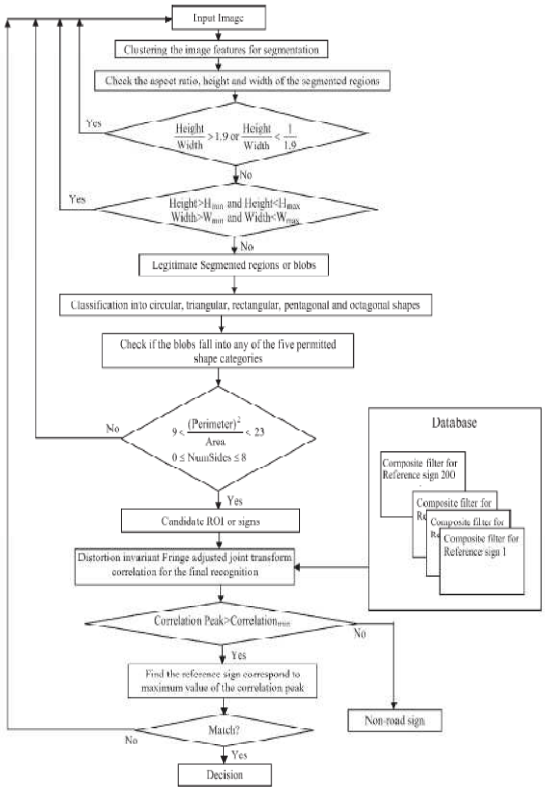

Fig 1. Flow chart of proposed algorithm

Segmentation

The use of color feature clustering to perform image segmentation , where it take into account the characteristic features related to the change in the color components.

Color Feature Extraction Using a Gabor Filter

The first step of segmentation is to measure the color features. To extract features, it compute the response of a Gabor filter oriented at the dominant direction of the neighborhood of a pixel. here use the International Commission on Illumination (CIE) L* a* b* representation of the color image because this color space can independently control color and intensity information [10]. The L* a* b* space consists of a luminosity layer *L**, a chromaticity layer *a** indicating where color falls along the red–green axis, and a chromaticity layer *b** indicating where the color falls along the blue–yellow axis. All of the color information is in the *a** and *b**layers, so that the color features are extracted from the *a** and *b**components. consider the local energy content of the *a** and *b** components as features for image segmentation.

Local energy is defined as the square root of the sum of the squared responses of two matched filters that have an identical amplitude spectrum but a different phase spectrum by 90◦.One filter has an even-symmetric line-spread function, and the other has an odd-symmetric line-spread function [11]. The local energy derived for the $a*$ component can be expressed as

$$LE^{a^*}(x,y) = \left(a^*(x,y) ** G_\theta^o(x,y)\right)^2 + \left(a^*(x,y) ** G_\theta^e(x,y)\right)^2 \quad (1)$$

where $G_\theta^o(x,y)$ and $G_\theta^e(x,y)$ are the pair of odd- and even symmetric filters. The even- and odd-symmetric filters are the real and imaginary parts, respectively, of the complex Gabor filter $G_\theta(x,y)$. Similarly, we can obtain the local energy measurement for the color component *b**.

For feature extraction purposes, it employ a Gabor filter oriented at an angle, which is adaptively chosen for each pixel. The 2-D circular Gabor filter can be defined as follows:

$$G_{f,\theta,\phi,\sigma}(x,y) = e^{-x^2+y^2 \,/\, 2\sigma^2} e^{j(2\Pi f(x\cos\theta + y\sin\theta)+\phi)} \quad (2)$$

where *f* is the spatial frequency of the cosine factor, θ is the orientation of the normal to the parallel stripes, φ is the phase offset, and the standard deviation σ of the Gaussian factor determines the (linear) size of the support of the Gabor function. Now, the size of the filter can be related to the standard deviation σ of the Gaussian factor as $w = 2\sigma + 1$. At each pixel, here choose a fixed value of size *w*, frequency *f*, and phase φ and a customized value of orientation θ at which the gradients in the local neighborhood possess a dominant direction. It conduct trials on several images to choose the optimum values of *w*, *f*, and φ, the Gabor filter used in this paper can be expressed as follows:

$$G_\theta(x,y) = e^{\frac{x^2+y^2}{18}} (\cos(0.2\Pi(x\cos\theta + y\sin\theta)) + j\sin(0.2\Pi(x\cos\theta + y\sin\theta))) \quad (3)$$

The orientation of the Gabor filter is determined based on the Idea of utilizing the information that is present in the horizontal and vertical gradients, i.e, ∇ x and ∇ y, respectively. Both gradients are derived by applying the *gradient* operator on the image. The orientation angle at pixel (*x*, *y*) is determined by following the approach i.e,,

$$\theta_k(x, y) = 90° + \frac{1}{2}\tan^{-1}\left(\frac{2g_{xy}}{g_{xx} - g_{yy}}\right) \quad (4)$$

where the definitions of *gxy*, *gxx*, and *gyy* are

$$g_{xy} = \sum_{p=x-(k-1)}^{x+(k-1)} \sum_{q=y-(k-1)}^{y+(k-1)} \nabla_x(p,q)\nabla_y(p,q)$$

$$g_{xx} = \sum_{p=x-(k-1)}^{x+(k-1)} \sum_{q=y-(k-1)}^{y+(k-1)} \nabla^2{}_x(p,q)$$

$$g_{yy} = \sum_{p=x-(k-1)}^{x+(k-1)} \sum_{q=y-(k-1)}^{y+(k-1)} \nabla^2{}_y(p,q)$$

K-Mean clustering

For clustering, here represents an image of *K* levels by encoding the pixel–cluster relationships, where each pixel value is replaced by the cluster label deduced by the *K*-means algorithm. At this stage, the clustered image is spatially smoothed by the repeated application of a 3 × 3 mode filter until the number of pixels that are different between images in two successive iterations is less than 1%. The mode filter yields an output equal to the value that occurs most often in the 3 × 3 window. In the smoothed image, there may be some regions of a few pixels located inside another large region.

At this stage, all the blobs in the segmented image are inspected in a verification process, and some of them are discarded according to their size and aspect ratio (i.e., the height-to-width ratio). Knowing the focal length of the camera, here require to impose some limits on the size of the objects, The limits for both criteria, i.e., size and aspect ratio, are empirically derived by a trial-and-error method based on the experiments on the images. The thresholds for the size criterion are selected at specific percentages with respect to the dimension of the images being analyzed. In considering the aspect ratio, blobs with an aspect ratio of greater than 1.9 and less than 1/1.9 are rejected.

Once the segmentation process is completed, easily obtain the ROIs or, in other words, possible candidate traffic signs.Fig. 2 shows the segmentation results for three test images.

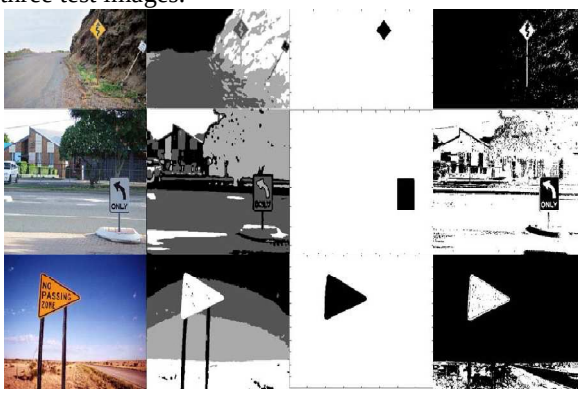

Fig. 2.Segmentation result. First column: Original images. Second column: Segmented images. Third column: Candidate ROIs. Fourth column: Segmentation results of the method in[7]

Shape Classification

The blobs that are obtained from the segmentation stage are verified in this stage according to their shape using two basic properties of a polygon, e.g. the ratio between the square of the perimeter and the area, and the number of sides. Any traffic-sign shape should fall into any of the following shape categories such as circular, rectangular, triangular. Any particular shape has a unique value of the parameter *Perimeter*2*/Area*, which is a constant for that shape. This parameter is named *Peri*2*Area*. Additionally, the number of sides is a standard attribute to distinguish among different polygonal shapes, and it is named *NumSides*. Both these features have the inherent characteristic of being independent of translation, scaling, and 2-D rotation of an image and would not only help identify the correct shape but also help reject the false objects (for example, cars and buildings) that are still present in the segmented image as candidate ROIs.

Shapes	**Circular**	**Triangular**	**Rectangular**
Synthetically Generated Shapes	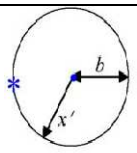	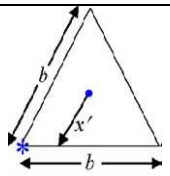	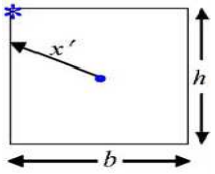
Plot For X’	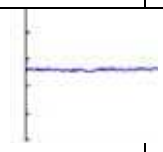	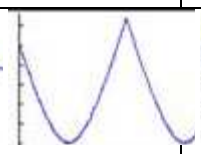	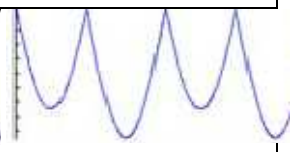
Numsides	0	3	4
Peri2area	$\frac{(2\prod b)^2}{\prod b^2}$	$\frac{(3b)^2}{\frac{1}{2}bh}$	$\frac{(2(b+h))^2{}^2}{bh}$

Table I shows all the shapes used for the purpose of road traffic control. In this table, the shapes are labeled with their dimensions. The values of *Peri*2*Area* and *NumSides* for the shapes are also given in Table I.

Distortion-Invariant Fringe-Adjusted Joint Transmission Correlation

JTC is one of the major techniques of pattern recognition. In JTC, the unknown input scene $s(x, y)$ and the known reference image $r(x, y)$ are displayed side-by-side in the input plane known as the input joint image, which is Fourier transformed. The Fourier-transformed patterns constructively interfere with each other to create an interference pattern called joint power spectrum (JPS). The JPS is inverse Fourier transformed to yield the correlation output. For a match, two correlation peaks or bright spots are produced, and for a mismatch, negligible numbers of or no correlation peaks are produced. In FJTC, the JPS is multiplied by a filter called fringe-adjusted filter before applying the inverse Fourier transform. For the distortion-invariant FJTC technique, the reference image $r(x, y)$ is synthesized from a set of training images.

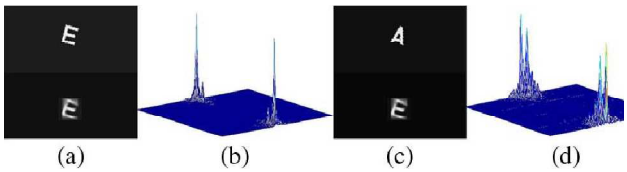

Fig.3(a) Input joint image with the desired target (the target is at the top, and the reference is at the bottom). (b) Correlation output. (c) Input joint image with the nontarget (the nontarget is at the top, and the reference is at the bottom).(d) Correlation output

To analyze the performance of distortion-invariant FJTC for a target in the input scene, a distorted binary input image such as a rotated English alphabet "E" has been taken as the target, which is placed at the top of the input joint image, as shown in Fig. 3(a). Now, the previously generated SDF for the alphabet "E," i.e., *r* SDF, is placed at the bottom of the same input joint image as the reference image, which is shown in Fig. 3(a). The simulation for FJTC has been performed with Fourier plane image subtraction to avoid the zero-order terms and unwanted false alarms. From the correlation output of Fig. 3(b) for the joint input image in Fig. 3(a), it is observed that there is a pair of cross correlation peaks indicating the presence of the target. There are two cross-correlation peaks, where the second one is at the mirror position of the first one. Locations of these correlation peaks actually depend on the relative placement of the input and reference images in the joint image. The same analysis has been made with a rotated non target image "A" with the same SDF previously generated for the alphabet "E" as the reference image, which is shown in Fig. 3(c). As given in Fig. 3(d), a pair of cross-correlation peaks is obtain for the non target but with negligible peak intensity. For the classification problem of propose work is the value of this peak intensity, which evaluates the discrimination ability of a correlation technique.

In addition to the absolute value of the correlation peak, we propose the metric primary-to-secondary peak ratio (PSR) to

evaluate the goodness of the matching between the target and reference images. The primary peak represents the maximum

cross-correlation peak intensity for the reference and the target. The secondary peak denotes the peak value after the cross correlation values in a small neighborhood around the primary peak location are made zero; thus, it can be considered as a peak resulting from the clutter that is present in the unknown input scene.

To find the sign that matches the best with a detected ROI from the database of reference signs, FJTC is applied only to the intensity component and not to all the three color components. As an alternative, FJTC could be employed to the three color components separately. In that case, for each reference sign, three composite filters should be computed offline corresponding to the three color components, and these three composite filters of any reference sign should be correlated with those of the unknown ROI independently. The final correlation output for an unknown ROI corresponding to any reference sign would then be considered as the summation of the correlation outputs from the three color channels. In this propose work with 70 Indian road sign images, the similarity search performance of distortion invariant FJTC with the intensity component has been found to be good to the same extent in comparison with the three color components. Additionally, there is a one-third reduction in the computation time, and only one composite filter has to be computed offline for each reference sign instead of three composite filters for the three color channels.

In this paper the utilization of the correlation output that is yielded from distortion-invariant FJTC for decision purposes about classifying the detected ROIs. For any candidate ROI, if the cross-correlation peak height is less than a predefined threshold CORR min, then that ROI is not considered as a road sign and, hence, is rejected. The value of the threshold CORR min is computed offline. To determine the value of this threshold, all the composite filters corresponding to the reference road signs in the database have been correlated with each other, and the minimum value among those correlation peaks is set for the threshold CORR min. If the final correlation peak is greater than the predefined threshold CORR min, then that ROI is classified as the reference sign for which it gives the highest

cross-correlation peak intensity; otherwise, that ROI is classified as a non road-sign object.

Fig. 4 some examples of road signs which is use for database.

Conclusion

The segmentation-based detection algorithm is found to be robust for its ability to mark a road sign as an ROI. Then, the shape classification algorithm improves the computation time in the next stage of recognition and rejects the non traffic-sign objects of similar colors as traffic signs (for example, cars and buildings) with a high probability .Followed by the preliminary detection, a classification/recognition segment deals only with the ROIs that are denoted as potential candidate regions. The distortion-invariant FJTC-based matching algorithm has excellent discrimination ability between target and non target objects. The FJTC technique yields sharper and stronger correlation peaks for the desired target than for the other non target objects, decides unerringly about an ROI to be a road sign or clutter, and then correctly classifies it from the known reference signs. The existing known difficulties for object recognition in outdoor environments have been handled by employing translation-, scale, and rotation-invariant shape classification processing and distortion-invariant correlation technique. Experiments have shown accurate sign detection and recognition performance. The presented algorithm is found to be robust and efficient to evaluate the signaling of the road for the maintenance of the traffic signs. Additionally, the whole developed system can be useful to help in the recognition and tracking of the road signs when the same sign will appear in several images. The generality of this automatic system makes it applicable to a wide range of computer vision tasks.

References

[1] N. Barnes, G. Loy, D. Shaw, and A. Robles-Kelly, “Regular polygon detection,” in *Proc. IEEE Conf. Comput. Vis.*, 2005, pp. 778–785.

[2] T. Ueta, Y. Sumi, N. Yabuki, and S. Matsumae, “A study on contour line and internal area extraction method by using the self-organization map,” in *Proc. Int. Symp. Intell. Signal Process. Commun. Syst.*, Tottori, Japan, 2006, pp. 685–688.

[3] G. Overett, L. Petersson, L. Andersson, and N. Pettersson, “Boosting a heterogeneous pool of fast hog features for pedestrian and sign detection,” in *Proc. Intell. Vehicles Symp.*, 2009, pp. 584–590.

[4] G. Loy and N. Barnes, “Fast shape-based road sign detection for a driver assistance system,” in *Proc. IEEE Conf. Int. Robots Syst.*, 2004,pp. 70–75.

[5] M. Benallal and J.Meunier, “Real-time color segmentation of road signs,” in *Proc. IEEE Can. Conf. Elect. Comput. Eng.*, 2003, pp. 1823–1826.

[6] A. Broggi, P. Cerri, P. Medici, P. Porta, and G. Ghisio, “Real time road signs recognition,” in *Proc. IEEE Intell. Vehicles Symp.*, 2007, pp. 981–986.

[7] S. Maldonado-Bascn, S. Lafuente-Arroyo, P. Gil-Jimnez, H. Gmez-Moreno, and F. Lpez-Ferreras, “Road-sign detection and recognition based on support vector machines,” *IEEE Trans. Intell. Transp. Syst.*, vol. 8, no. 2, pp. 264–278, Jun. 2007

[8] A. Escalera and L. Moreno, “Road traffic sign detection and classification,” *IEEE Trans. Ind. Electron.*, vol. 44, no. 6, pp. 847–859, Dec. 1997.

[9] V. Andrey and J. Kang-Hyun, “Automatic detection and recognition of traffic signs using geometric structure analysis,” in *Proc. SICE-ICASE Int. Joint Conf.*, 2006, pp. 1451–1456.

[10] L. Guibert, Y. Petillot, and J. Tocnaye, “Real-time demonstration of an on-board nonlinear joint transform correlator system,” *Opt. Eng.*, vol. 36, no. 3, pp. 820–824, Mar. 1997

[11] H. Cheng, X. Jiang, Y. Sun, and J. Wang, “Color image segmentation: Advances and prospects,” *Pattern Recognit.*, vol. 34, no. 12, pp. 2259–2281, Dec. 2001.

[12] M. Morrone and D. Burr, “Feature detection in human vision: A phasedependent energy model,” *Proc. R. Soc. Lond.*, vol. 235, no. 1280, pp. 221–245, Dec. 1988.

[13] W. Shadeed, D. Abu-Al-Nadi, and M. Mismar, "Road traffic sign detection in color images," in *Proc. IEEE Int. Conf. Electron., Circuits Syst.*, 2003, pp. 890–893.
[14] V. Rehrmann and L. Priese, "Fast and robust segmentation of natural color scenes," in *Proc. 3rd Asian Conf. Comput. Vis.*, 1998, pp. 598–606.
[15] S. Escalera and P. Radeva, "Fast grey scale road sign model matching and recognition," in *Recent Advances in Artificial Intelligence Research and Development*. Amsterdam, The Netherlands: IOS, 2004, pp. 69–76.